Stark quenching of rovibrational states of H2+ due to motion in a magnetic field

Jean-Philippe Karr

Stark quenching of rovibrational states of H_2^+ due to motion in a magnetic field

Jean-Philippe Karr
Laboratoire Kastler Brossel,
Sorbonne Université, CNRS,
ENS-PSL Research University, Collège de France
4 place Jussieu, F-75005 Paris, France and
Université d'Evry-Val d'Essonne, Université Paris-Saclay,
Boulevard François Mitterrand, F-91000 Evry, France

The motional electric field experienced by an H_2^+ ion moving in a magnetic field induces an electric dipole, so that one-photon dipole transitions between rovibrational states become allowed. Field-induced spontaneous decay rates are calculated for a wide range of states. For an ion stored in a high-field ($B \sim 10$ T) Penning trap, it is shown that the lifetimes of excited rovibrational states can be shortened by typically 1-3 orders of magnitude by placing the ion in a large cyclotron orbit. This can greatly facilitate recently proposed [E. G. Myers, Phys. Rev. A **98**, 010101 (2018)] high-precision spectroscopic measurements on H_2^+ and its antimatter counterpart for tests of CPT symmetry.

Introduction

The hydrogen molecular ions, H_2^+ and its isotopes (HD^+, D_2^+) have long since been identified as a highly promising system for fundamental physics tests. High-precision spectroscopy of rovibrational transitions can be used to determine the proton-electron and deuteron-electron mass ratios [1, 2] and probe their possible time variation [3–5]. Furthermore, measuring an appropriate set of transitions in H_2^+ and HD^+ would allow a determination of the proton and deuteron charge radii and the Rydberg constant [6] and thus may contribute to resolving the existing discrepancies on their values [7–11]. Spectroscopy of H_2^+ compared with its antimatter counterpart $\bar{H}_2^-$ was recently proposed for improved tests of CPT symmetry [12].

Theoretical predictions of rovibrational transition frequencies have surpassed the 10^{-11} accuracy level [13] which already allows for an improved determination of mass ratios [14, 15]. In HD^+, experiments with ultracold trapped ions have reached a precision of 10^{-9} [16, 17] and more recently 5×10^{-10} [18]. Studies on H_2^+ [19–23] have been so far performed by different techniques yielding lower accuracies. The main obstacle faced by ultrahigh-resolution spectroscopy of trapped H_2^+ (or $\bar{H}_2^-$) is quantum state preparation, due to the fact that, unlike in the heteronuclear HD^+, rovibrational transitions are not dipole-allowed. As a result, rovibrational states of vibration quantum number $v \geq 1$ have very long lifetimes typically of the order of 10 days [24, 25]. It would take several months for an ion produced in e.g. $v = 10$ to decay down to $v = 0$. Pure rotational transitions for lower values of rotational quantum number L are even slower, the rotational levels of $v = 0$ with $L < 8$ having lifetimes greater than one year, for example. In addition, optical pumping methods for cooling the internal degrees of freedom [26] are not available. One solution [27] consists in creating the ions directly in the desired rovibrational state by state-selective multiphoton ionization (REMPI) of H_2 [28, 29]. However, no selective production scheme is available for antimatter $\bar{H}_2^-$ ions [12]. Rovibrational cooling by cold He buffer gas has also been proposed [30] but is again not well suited for antimatter ions.

In this paper, we study another rovibrational relaxation process relevant for experiments performed in a Penning trap, first proposed in [12]. The idea is to exploit the motional electric field experienced by an ion as it moves in a magnetic field. This electric field polarizes the ion [31] making one-photon ro-vibrational decay allowed. The Stark quenching process is much less efficient in H_2^+ as e.g. for the 2S state in hydrogen [32] because the mixing of $1s\sigma_g$ rovibrational states induced by the electric field occurs with excited electronic states and is very weak. Nevertheless, our results show that rovibrational decay can typically be accelerated by at least one order of magnitude in a high-field ($B \sim 10$ T) Penning trap.

In the following, we present the calculation of decay rates for a wide range of rovibrational states. The paper is structured as follows : the theoretical expression of the decay rate is derived in Sec. I. The numerical method is described in Sec. II. Results are presented in Sec. III, and their experimental implications briefly discussed.

I. THEORY

A. Motional electric field

We consider an H_2^+ ion in a Penning trap with a uniform magnetic field $\mathbf{B_0}$ along the z axis, placed in a cyclotron orbit of radius r_c. The ion's velocity is

$$\mathbf{v}(t) = \frac{qB_0 r_c}{m} \left[\sin(\omega_c t)\mathbf{e_x} + \cos(\omega_c t)\mathbf{e_y}\right] \tag{1}$$

where $\omega_c = qB_0/m$ is the cyclotron frequency. The moving ion experiences a motional electric field

$$\mathbf{E_0}(t) = \mathbf{v}(t) \times \mathbf{B_0} = E_0 \left[\cos(\omega_c t)\mathbf{e_x} - \sin(\omega_c t)\mathbf{e_y}\right] \tag{2}$$

with $E_0 = qB_0^2 r_c/m$. This electric field can be expressed in terms of the standard polarizations

$$\boldsymbol{\epsilon}_{\pm 1} = \mp \frac{1}{\sqrt{2}} \left(\mathbf{e_x} \pm i\mathbf{e_y}\right). \tag{3}$$

One gets :

$$\mathbf{E_0}(t) = \frac{E_0}{\sqrt{2}} \left(e^{-i\omega_c t}\boldsymbol{\epsilon}_{-1} + h.c.\right). \tag{4}$$

Decay induced by the field $\mathbf{E_0}(t)$ can be understood as a two-photon process whereby a "cyclotron" photon of energy $\hbar\omega_c$ is emitted (or absorbed) and another is spontaneously emitted. Since the cyclotron frequency is very small with respect to rovibrational transition frequencies in H_2^+, one may approximate $\mathbf{E_0}(t)$ by a static field

$$\mathbf{E_0} = \frac{E_0}{\sqrt{2}} \left(\boldsymbol{\epsilon}_{-1} - \boldsymbol{\epsilon}_1\right). \tag{5}$$

B. Dipole matrix elements

A ro-vibrational state (v, L) of H_2^+ supported by the ground $(1s\sigma_g)$ electronic curve will be mixed by the motional electric field with states of opposite parity supported by excited electronic curves. At the first order of perturbation theory, the perturbed wavefunction may be written as

$$\left|\psi^{(1)}_{v,L,M}\right\rangle = \left|\psi_{v,L,M}\right\rangle + \frac{1}{E_{v,L} - H}\mathbf{d} \cdot \mathbf{E_0} \left|\psi_{v,L,M}\right\rangle \tag{6}$$

As a result, one-photon transitions between ro-vibrational states become dipole-allowed. Keeping only leading-order terms, the transition dipole moment is

$$\begin{aligned}\left\langle\psi^{(1)}_{v',L',M'}\right| \mathbf{d}\cdot\boldsymbol{\epsilon} \left|\psi^{(1)}_{v,L,M}\right\rangle \;=\; E_0 \Bigg(&\left\langle\psi_{v',L',M'}\right| \mathbf{d}\cdot\boldsymbol{\epsilon} \frac{1}{E_{v,L} - H}\mathbf{d}\cdot\boldsymbol{\epsilon}_0 \left|\psi_{v,L,M}\right\rangle \\ &+ \left\langle\psi_{v',L',M'}\right| \mathbf{d}\cdot\boldsymbol{\epsilon}_0 \frac{1}{E_{v',L'} - H}\mathbf{d}\cdot\boldsymbol{\epsilon} \left|\psi_{v,L,M}\right\rangle\Bigg)\end{aligned} \tag{7}$$

where $\boldsymbol{\epsilon}_0 = (\boldsymbol{\epsilon}_{-1} - \boldsymbol{\epsilon}_1)/\sqrt{2}$. This can be written in terms of the two-photon transition operator $Q_{\boldsymbol{\epsilon}_1\boldsymbol{\epsilon}_2}(\omega_1, \omega_2)$ [33, 34] :

$$\left\langle\psi^{(1)}_{v',L',M'}\right| \mathbf{d}\cdot\boldsymbol{\epsilon} \left|\psi^{(1)}_{v,L,M}\right\rangle = E_0 \left\langle\psi_{v',L',M'}\right| Q_{\boldsymbol{\epsilon}_0\boldsymbol{\epsilon}}(0,\omega) \left|\psi_{v,L,M}\right\rangle, \tag{8}$$

where $\hbar\omega = E_{v,L} - E_{v',L'}$, and

$$Q_{\boldsymbol{\epsilon}_1\boldsymbol{\epsilon}_2}(\omega_1, \omega_2) \;=\; Q_{\boldsymbol{\epsilon}_2\boldsymbol{\epsilon}_1}(\omega_1) + Q_{\boldsymbol{\epsilon}_1\boldsymbol{\epsilon}_2}(\omega_2), \tag{9}$$

$$Q_{\boldsymbol{\epsilon}_2\boldsymbol{\epsilon}_1}(\omega_1) \;=\; \mathbf{d}\cdot\boldsymbol{\epsilon}_2 \frac{1}{E_{v,L} - \hbar\omega_1 - H}\mathbf{d}\cdot\boldsymbol{\epsilon}_1 \tag{10}$$

C. Properties of the two-photon transition operator

Since this operator couples twice the vector operator **d**, it may be written as a sum of operators of rank 0, 1 and 2. Furthermore, one can decompose it into its symmetrical and antisymmetrical parts [33]

$$Q_{\boldsymbol{\epsilon}_1\boldsymbol{\epsilon}_2}(\omega_1,\omega_2) = Q^S_{\boldsymbol{\epsilon}_1\boldsymbol{\epsilon}_2}(\omega_1,\omega_2) + Q^A_{\boldsymbol{\epsilon}_1\boldsymbol{\epsilon}_2}(\omega_1,\omega_2), \tag{11}$$

$$Q^S_{\boldsymbol{\epsilon}_1\boldsymbol{\epsilon}_2}(\omega_1,\omega_2) = \frac{1}{2}\left(Q_{\boldsymbol{\epsilon}_1\boldsymbol{\epsilon}_2}(\omega_1,\omega_2) + Q_{\boldsymbol{\epsilon}_2\boldsymbol{\epsilon}_1}(\omega_1,\omega_2)\right) \tag{12}$$

$$Q^A_{\boldsymbol{\epsilon}_1\boldsymbol{\epsilon}_2}(\omega_1,\omega_2) = \frac{1}{2}\left(Q_{\boldsymbol{\epsilon}_1\boldsymbol{\epsilon}_2}(\omega_1,\omega_2) - Q_{\boldsymbol{\epsilon}_2\boldsymbol{\epsilon}_1}(\omega_1,\omega_2)\right). \tag{13}$$

Then $Q^S_{\boldsymbol{\epsilon}_1\boldsymbol{\epsilon}_2}(\omega_1,\omega_2)$ is decomposed into operators of ranks 0 and 2, while $Q^A_{\boldsymbol{\epsilon}_1\boldsymbol{\epsilon}_2}(\omega_1,\omega_2)$ is of rank 1.

Selection rules for Stark-induced decay are thus identical to those of two-photon transitions [35], i.e. $\Delta L = 0, \pm 2$ for rovibrational transitions within the $1s\sigma_g$ electronic state. $L = 0 \to L' = 0$ transitions only involve the scalar component of the two-photon operator, while $L \to L \pm 2$ transitions only involve the rank 2 component. The $L \to L$ transitions with $L \geq 1$ are the most complicated cases, involving all three terms (rank 0, 1 and 2).

We define the scalar ($Q^{(0)}$) and tensor ($Q^{(2)}$) operators appearing in the decomposition of $Q^S_{\boldsymbol{\epsilon}_1\boldsymbol{\epsilon}_2}$ by the relationship

$$Q^S_{00} = Q^{(0)}_0 + Q^{(2)}_0 \tag{14}$$

The required $Q^S_{q_1q_2}$ components can then be expressed in terms of irreducible components $Q^{(0)}_q$, $Q^{(2)}_q$. One obtains [5]

$$Q^S_{\pm1\pm1} = \sqrt{\frac{3}{2}}Q^{(2)}_{\pm2} \tag{15}$$

$$Q^S_{\pm10} = \frac{\sqrt{3}}{2}Q^{(2)}_{\pm1} \tag{16}$$

$$Q^S_{\pm1\mp1} = -Q^{(0)}_0 + \frac{1}{2}Q^{(2)}_0 \tag{17}$$

Similarly, for the antisymmetrical part $Q^A_{\boldsymbol{\epsilon}_1\boldsymbol{\epsilon}_2}$ we define the vector operator $Q^{(1)}$ by the relationship

$$Q^A_{-10} = Q^{(1)}_{-1} \tag{18}$$

and the $Q^A_{q_1q_2}$ components can be expressed in terms of irreducible components $Q^{(1)}_q$ [33]

$$Q^A_{\pm10} = \mp Q^{(1)}_{\pm1} \tag{19}$$

$$Q^A_{\pm1\mp1} = \mp Q^{(1)}_0 \tag{20}$$

Finally, we set

$$Q_s = \frac{\langle v'L'||Q^{(0)}||vL\rangle}{\sqrt{2L'+1}} \tag{21}$$

$$Q_v = \frac{\langle v'L'||Q^{(1)}||vL\rangle}{\sqrt{2L'+1}} \tag{22}$$

$$Q_t = \frac{\langle v'L'||Q^{(2)}||vL\rangle}{\sqrt{2L'+1}}. \tag{23}$$

D. Decay rates

The decay rate (or Einstein coefficient A) of a given state (v, L, M) associated with a transition towards a state (v', L') (in s^{-1}) is given by

$$A_{v,L,M,v',L'} = \frac{2\omega^3}{3\epsilon_0 hc^3} \sum_{M',\boldsymbol{\epsilon}} \left|\langle\psi_{v'L'M'}|\,\mathbf{d}\cdot\boldsymbol{\epsilon}\,|\psi_{v,L,M}\rangle\right|^2 \tag{24}$$

In the usual case of spontaneous emission in an isotropic environment, the decay rate does not depend on M, but here anisotropy arises from the fact that the electric field $\mathbf{E_0}$ is polarized perpendicularly to the z axis.
In the simplest case $L = L' = 0$ we get

$$A_{v,L=0,M=0,v',L'=0} = \frac{2\omega^3}{3\epsilon_0 hc^3} E_0^2 Q_s^2. \tag{25}$$

For $L' = L \pm 2$:

$$\begin{aligned}
A_{v,L,M,v',L'} &= \frac{2\omega^3}{3\epsilon_0 hc^3}\frac{E_0^2}{2}\sum_{M',q}\left(\left|\langle v'L'M'|\, Q^S_{-1q}(0,\omega)\,|vLM\rangle\right|^2 + \left|\langle v'L'M'|\, Q^S_{1q}(0,\omega)\,|vLM\rangle\right|^2\right) \\
&= \frac{\omega^3}{3\epsilon_0 hc^3}E_0^2\left\{\frac{3}{2}\left|\langle v'L'M+2|\, Q^{(2)}_2\,|vLM\rangle\right|^2 + \frac{3}{2}\left|\langle v'L'M-2|\, Q^{(2)}_{-2}\,|vLM\rangle\right|^2\right. \\
&\quad \left. +\frac{3}{4}\left|\langle v'L'M+1|\, Q^{(2)}_1\,|vLM\rangle\right|^2 + \frac{3}{4}\left|\langle v'L'M-1|\, Q^{(2)}_{-1}\,|vLM\rangle\right|^2 + \frac{1}{2}\left|\langle v'L'M|\, Q^{(2)}_0\,|vLM\rangle\right|^2\right\} \\
&= \frac{\omega^3}{3\epsilon_0 hc^3}E_0^2\left\{\frac{3}{2}\left|\langle LM22|L'M+2\rangle\right|^2 + \frac{3}{2}\left|\langle LM2-2|L'M-2\rangle\right|^2\right. \\
&\quad \left. +\frac{3}{4}\left|\langle LM21|L'M+1\rangle\right|^2 + \frac{3}{4}\left|\langle LM2-1|L'M-1\rangle\right|^2 + \frac{1}{2}\left|\langle LM20|L'M\rangle\right|^2\right\} Q_t^2
\end{aligned} \tag{26}$$

One can show that the averaged decay rate $\bar{A}_{v,L,v',L'} = \left(\sum_{M=-L}^{L} A_{v,L,M,v',L'}\right)/(2L+1)$ is

$$\bar{A}_{v,L,v',L'} = \frac{\omega^3}{3\epsilon_0 hc^3}E_0^2 Q_t^2 \frac{2L'+1}{2L+1}. \tag{27}$$

Finally, for $L' = L \geq 1$ the spontaneous emission rate is

$$\begin{aligned}
A_{v,L,M,v',L} &= \frac{2\omega^3}{3\epsilon_0 hc^3}E_0^2\sum_{M'}\left|\langle v'LM'|Q^S_{\boldsymbol{\epsilon}_0\boldsymbol{\epsilon}}(0,\omega)|vLM\rangle + \langle v'LM'|Q^A_{\boldsymbol{\epsilon}_0\boldsymbol{\epsilon}}(0,\omega)|vLM\rangle\right|^2 \\
&= \frac{2\omega^3}{3\epsilon_0 hc^3}\frac{E_0^2}{2}\sum_{M',q}\left|\langle v'LM'|\, Q^S_{-1q}\,|vLM\rangle + \langle v'LM'|\, Q^S_{1q}\,|vLM\rangle\right. \\
&\quad \left. + \langle v'LM'|\, Q^A_{-1q}\,|vLM\rangle + \langle v'LM'|\, Q^A_{1q}\,|vLM\rangle\right|^2 \\
&= \frac{\omega^3}{3\epsilon_0 hc^3}E_0^2\left\{\frac{3}{2}\left(\left|\langle LM22|LM+2\rangle\right|^2 + \left|\langle LM2-2|LM-2\rangle\right|^2\right)Q_t^2\right. \\
&\quad + \left|\frac{\sqrt{3}}{2}\langle LM21|LM+1\rangle\, Q_t - \langle LM11|LM+1\rangle\, Q_v\right|^2 \\
&\quad + \left|\frac{\sqrt{3}}{2}\langle LM2-1|LM-1\rangle\, Q_t + \langle LM1-1|LM-1\rangle\, Q_v\right|^2 \\
&\quad + \left|-Q_s + \frac{1}{2}\langle LM20|LM\rangle\, Q_t + \langle LM10|LM\rangle\, Q_v\right|^2 \\
&\quad \left. + \left|-Q_s + \frac{1}{2}\langle LM20|LM\rangle\, Q_t - \langle LM10|LM\rangle\, Q_v\right|^2\right\}
\end{aligned} \tag{28}$$

The averaged decay rate is

$$\bar{A}_{v,L,v',L} = \frac{\omega^3}{3\epsilon_0 hc^3}E_0^2\left(2Q_s^2 + Q_t^2 + \frac{4}{3}Q_v^2\right). \tag{29}$$

II. NUMERICAL METHOD

We now present the calculation of two-photon reduced matrix elements. Our numerical method has been previously described in Refs. [5, 35, 36], and we briefly recall the main points here. The three-body Schrödin-

ger equation is solved using the following variational expansion of the wave function :

$$\begin{aligned}\Psi_{LM}(\mathbf{r}_1,\mathbf{r}_2) &= \sum_{l_1+l_2=L} \mathcal{Y}^{l_1 l_2}_{LM}(\mathbf{r}_1,\mathbf{r}_2) R^L_{l_1 l_2}(r_1,r_2,r_{12}),\\ R^L_{l_1 l_2}(r_1,r_2,r_{12}) &= \sum_{n=1}^{N_{l_1}} \Big\{ C_n \,\mathrm{Re}\big[e^{-\alpha_n r_{12}-\beta_n r_1-\gamma_n r_2}\big] + D_n \,\mathrm{Im}\big[e^{-\alpha_n r_{12}-\beta_n r_1-\gamma_n r_2}\big]\Big\}.\end{aligned} \tag{30}$$

r_1, r_2, r_{12} are the interparticle distances, and $\mathcal{Y}^{l_1 l_2}_{LM}(\mathbf{r}_1,\mathbf{r}_2) = r_1^{l_1} r_2^{l_2} Y^{l_1 l_2}_{LM}(\hat{\mathbf{r}}_1,\hat{\mathbf{r}}_2)$ where $Y^{l_1 l_2}_{LM}$ is a bipolar spherical harmonic. The complex exponents α_n, β_n, γ_n are generated pseudorandomly in several intervals. All parameters, i.e. interval bounds and the number of basis functions N_{i,l_1} in each interval i and angular momentum subset $\{l_1, l_2\}$ (keeping the total basis length $N = 2\sum_{i,l_1} N_{i,l_1}$ constant), have been optimized for a few tens of states. This yielded accuracies of 10^{-12} a.u. or better on the energy levels of all 201 rovibrational levels considered here using basis lengths $N = 2000 - 3500$.

For the calculation of two-photon matrix elements, the following three terms, which correspond to the possible values L'–1, L'+1, L' for the angular momentum of the intermediate state, are evaluated numerically :

$$a_{0,\pm} = \frac{1}{\sqrt{(2L+1)(2L'+1)}} \left[\langle v'L'\|\mathbf{d}(E_{vL} - H_{L''})^{-1}\mathbf{d}\|vL\rangle + \langle v'L'\|\mathbf{d}(E_{v'L'} - H_{L''})^{-1}\mathbf{d}\|vL\rangle\right] \tag{31}$$

where $H_{L''}$ denotes the restriction of the Schrödinger Hamiltonian H to a subspace of angular momentum L'', and a_0, a_+, a_- respectively correspond to $L'' = L', L'+1, L'-1$. Basis lengths $N_{L''} = 2000 - 3000$ are typically used for $H_{L''}$ which is more than sufficient to obtain these quantities with five significant digits. The reduced matrix elements of $Q^{(k)}$ are related to a_-, a_+, a_0 in the following way :

$$\frac{\langle v'L\|Q^{(0)}\|vL\rangle}{\sqrt{2L+1}} = \frac{1}{3}\left(a_- + a_0 + a_+\right) \tag{32}$$

$$\frac{\langle v'L\|Q^{(1)}\|vL\rangle}{\sqrt{2L+1}} = \sqrt{L(L+1)}\left[\frac{a_-}{L} + \frac{a_0}{L(L+1)} - \frac{a_+}{L+1}\right] \tag{33}$$

$$\frac{\langle v'L+2\|Q^{(2)}\|vL\rangle}{\sqrt{2L+5}} = -\sqrt{\frac{2(2L+1)}{3(2L+3)}}\, a_- \tag{34}$$

$$\frac{\langle v'L\|Q^{(2)}\|vL\rangle}{\sqrt{2L+1}} = -\frac{1}{3}\sqrt{(2L+3)(2L-1)L(L+1)}\left[\frac{a_-}{L(2L-1)} - \frac{a_0}{L(L+1)} + \frac{a_+}{(2L+3)(L+1)}\right] \tag{35}$$

$$\frac{\langle v'L-2\|Q^{(2)}\|vL\rangle}{\sqrt{2L-3}} = -\sqrt{\frac{2(2L+1)}{3(2L-1)}}\, a_+ \tag{36}$$

III. RESULTS AND DISCUSSION

The range of ro-vibrational states was chosen in order to provide all the results relevant to any of the following experimental situations :

(i) H_2^+ ions produced by electron-impact ionization of H_2. This process has been shown to create ions predominantly in $v = 0-12$, $L = 0-4$ with only ~ 1 percent probability of populating higher vibrational states [37].

(ii) $\bar{H}_2^-$ antimatter ions produced through the reaction $\bar{H}^+ + \bar{p} \to \bar{H}_2^- + e^+$, as proposed in [12], using $\bar{H}^+$ ions to be produced in the GBAR experiment [38]. The reaction being exothermic by 1.896 eV, the $\bar{H}_2^-$ ion will be produced with $v = 0-8$ and $L = 0-27$, with low-v, high L states being favored.

The two-photon matrix elements Q_s, Q_v and Q_t were calculated for all the required states [39]. The corresponding M-averaged decay rates $A/(B_0^4 r_c^2)$ in $\mathrm{s^{-1}T^{-4}mm^{-2}}$ are given in the following Tables for $L \to L' = L-2$ ($\Delta v = v - v' = 0, 1, 2$, Tables I-III), $L \to L' = L$ ($\Delta v = 1, 2$, Tables IV-V), and $L \to L' = L+2$ transitions ($\Delta v = 1, 2$, Tables VI-VII). The total decay rates $\bar{A}_{v,L} = \sum_{v',L'} \bar{A}_{v,L,v',L'}$ are given in Table VIII.

The decay rates decrease sharply with increasing Δv, as previously observed in the case of two-photon transitions [40]. Decay towards $v' = v-3$ states was also included in the total rates of Table VIII. However, since the fractional contribution of $\Delta v = 3$ transitions to the overall decay rates amounts to less than 10^{-3} in all cases, these decay rates are not reported here.

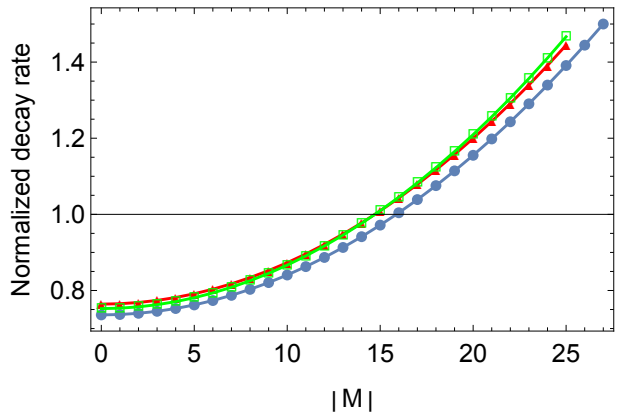

FIGURE 1: Normalized decay rate $A_{v,L,M,v',L'}/\bar{A}_{v,L,v',L'}$ for $L = 27, L' = 25$ (blue circles), $L = 25, L' = 27$ (red triangles), and $v = 1, L = 25, v' = 0, L' = 25$ (green squares). Note that the M dependence is independent of v and v' for $\Delta L = \pm 2$ (see Eq. (26)), but not for $\Delta L = 0$ (Eq. (28)).

The dependence of the decay rates on the magnetic quantum number M is illustrated in Fig. 1. One can see that the decay rate increases with $|M|$.

These results can be used to precisely model the time evolution of H_2^+ (or $\bar{H}_2^-$) ro-vibrational populations from initial conditions corresponding to different production schemes. Such a study is outside the scope of the present paper, but it is already possible to draw some qualitative conclusions. Fig. 2 shows both zero-field and Stark-quenched lifetimes of selected ro-vibrational states, for a magnetic field value $B_0 = 8.5$ T and a cyclotron radius $r_c = 2$ mm which correspond to the parameters of the Penning trap operated in Tallahassee [41].

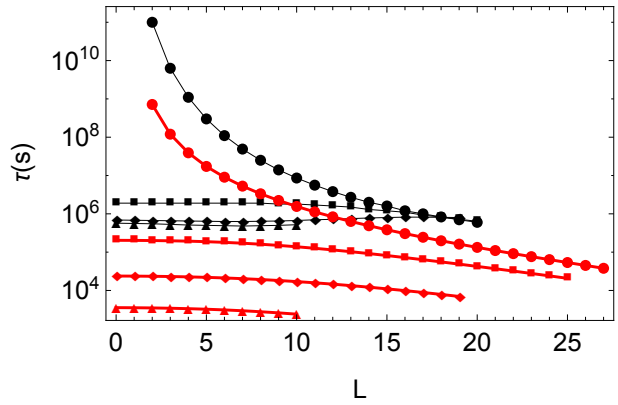

FIGURE 2: Stark lifetimes of H_2^+ rovibrational states for an ion in a cyclotron orbit of radius $r_c = 2$ mm in a magnetic field $B_0 = 8.5$ T are shown by thick red lines. For comparison, the zero-field lifetimes (taken from [24]) are shown by thin black lines. Circles, squares, diamonds and triangles respectively stand for $v = 0, 1, 4, 8$.

One may observe that Stark quenching is most efficient for excited vibrational states, leading to lifetimes of e.g. less than one hour for $v = 8$, a few hours for $v = 4$, and a few days for $v = 1$. This represents a reduction by 1-2 orders of magnitude with respect to the zero-field lifetime. Quenching of the vibrational motion down to $v = 0$ may thus be expected to occur within ~ 1 week in present-day Penning traps. Quenching of the rotational motion is significantly slower, with lifetimes ranging from ~ 10 hours for $(v = 0, L = 27)$ up to ~ 23 years for $(v = 0, L = 2)$. Thus for manipulation of antimatter molecular ions which may be formed in high-L states [12] it would be useful to transfer the ions to a larger trap where the ions could be placed in a cyclotron orbit of very large radius. For example, for $B_0 = 10$ T and $r_c = 20$ mm, the lifetimes would range from ~ 3 minutes for $(v = 0, L = 27)$ to ~ 7 days for $(v = 0, L = 3)$. Rotational quenching down to $L = 1$ or 2 could thus occur in about 1 week.

In conclusion, our results indicate that vibrational quenching of H_2^+ or its antimatter counterpart may be achieved within ~ 1 week in existing Penning trap apparatus, and that rotational quenching is achievable

over a similar time scale in a specially designed apparatus allowing for larger cyclotron radii. This opens new possibilities for ultra-high resolution spectroscopy of the simplest (anti)-molecule. Rovibrational Stark quenching of H_2^+ (and other homonuclear diatomic molecular ions) could also be significant if they are stored in heavy-ion storage rings in which the bending sections have comparably large values of $B_0^4 r_c^2$.

Finally, it is worth noting that, although we have focused on the case of an H_2^+ ion orbiting in an external magnetic field, the results presented here may readily be applied to calculate its decay rates in an external static electric field $\mathbf{E_0}$. Since the decay rate of a particular M state depends on the electric field polarization, Eqs. (26) and (28) have to be adapted to the specific case under study. However, the averaged decay rates are independent of the field polarization, so that Eqs. (25), (27), and (29) may be directly applied. The results of Tables I-VIII can also be directly exploited using the relationship $E_0 = qB_0^2 r_c/m$.

Acknowledgments

I thank E.G. Myers for bringing this problem to my attention and for stimulating discussions. I also thank him, as well as L. Hilico, for useful suggestions on the manuscript. I acknowledge support as a fellow of the Institut Universitaire de France.

[1] W.H. Wing, G.A. Ruff, W.E. Lamb, Jr., and J.J. Spezeski, Phys. Rev. Lett. **36**, 1488 (1976).
[2] B. Roth, J. Koelemeij, S. Schiller, L. Hilico, J.-Ph. Karr, V. I. Korobov, and D. Bakalov, Precision Physics of Simple Atoms and Molecules, ed. S. Karshenboim, Lectures Notes in Physics **745**, 205. (Springer-Verlag, Berlin, Heidelberg, 2008).
[3] S. Schiller and V Korobov, Phys. Rev. A **71**, 032505 (2005).
[4] S. Schiller, D. Bakalov, and V.I. Korobov, Phys. Rev. Lett. **113**, 023004 (2014).
[5] J.-Ph. Karr, J. Mol. Spectrosc. **300**, 37 (2014).
[6] J.-Ph. Karr, L. Hilico, J. C. J. Koelemeij, V.I. Korobov, Phys. Rev. A **94**, 050501(R) (2016).
[7] A. Antognini *et al.*, Science **339**, 417 (2013).
[8] J. Arrington and I. Sick, J. Phys. Chem. Ref. Data **44**, 031204 (2015).
[9] R. Pohl *et al.*, Science **353**, 669 (2016).
[10] A. Beyer *et al.*, Science **358**, 79 (2017).
[11] H. Fleurbaey, S. Galtier, S. Thomas, M. Bonnaud, L. Julien, F. Biraben, F. Nez, M. Abgrall, and J. Guéna, Phys. Rev. Lett. **120**, 183001 (2018).
[12] E.G. Myers, Phs. Rev. A **98**, 010101 (2018).
[13] V. I. Korobov, L. Hilico, J.-Ph. Karr, Phys. Rev. Lett. **118**, 233001 (2017).
[14] S. Sturm, F. Köhler, J. Zatorski, A. Wagner, Z. Harman, G. Werth, W. Quint, C.H. Keitel, and K. Blaum, Nature **467**, 506 (2014).
[15] F. Heiße, F. Köhler-Langes, S. Rau, J. Hou, S. Junck, A. Kracke, A. Mooser, W. Quint, S. Ulmer, G. Werth, K. Blaum, S. Sturm, Phys. Rev. Lett. **119**, 033001 (2017).
[16] U. Bressel, A. Borodin, J. Shen, M. Hansen, I. Ernsting, and S. Schiller, Phys. Rev. Lett. **108**, 183003 (2012).
[17] J. Biesheuvel, J.-Ph. Karr, L. Hilico, K.S.E. Eikema, W. Ubachs, and J.C.J. Koelemeij, Nature Comm. **7**, 10385 (2016).
[18] S. Alighanbari, M.G. Hansen, V.I. Korobov, and S. Schiller, Nat. Phys. **14**, 555 (2018).
[19] K.B. Jefferts, Phys. Rev. Lett. **23**, 1476 (1969).
[20] A. Carrington, C.A. Leach, R.E. Moss, T.C. Steimle, M.R. Viant, and Y.D. West, J. Chem. Soc. Faraday Trans. **89**, 603 (1993).
[21] A.D.J. Critchley, A.N. Hughes, and I.R. McNab, Phys. Rev. Lett. **86**, 1725 (2001).
[22] C. Haase, M. Beyer, C. Jungen, and F. Merkt, J. Chem. Phys. **142**, 064310 (2015).
[23] M. Beyer and F. Merkt, Phys. Rev. Lett. **116**, 093001 (2016).
[24] A.G. Posen, A. Dalgarno, and J.M. Peek, At. Data and Nucl. Data Tables **28**, 265 (1983).
[25] H. Olivares Pilón and D. Baye, J. Phys. B **45**, 065101 (2012).
[26] T. Schneider, B. Roth, H. Duncker, I. Ernsting, and S. Schiller, Nature Phys. **6**, 275 (2010).
[27] J.-Ph. Karr, A. Douillet, and L. Hilico, Appl. Phys. B **107**, 1043 (2012).
[28] S.L. Anderson, G.D. Kubiak, and R.N. Zare, Chem. Phys. Lett. **105**, 22 (1984).
[29] M.A. O'Halloran, S.T. Pratt, P.M. Dehmer, and J.L. Dehmer, J. Chem. Phys. **87**, 3288 (1987).
[30] S. Schiller, I. Kortunov, M. Hernández Vera, F. Gianturco, and H. da Silva, Jr., Phys. Rev. A **95**, 043411 (2017).
[31] J.K. Thompson, S.Rainville, and D.E. Pritchard, Nature **430**, 58 (2004).
[32] W.E. Lamb and R.C. Retherford, Phys. Rev. **79**, 549 (1950).
[33] G. Grynberg, Habilitation thesis, Université Pierre et Marie Curie (Paris 6) (1976).
[34] G. Grynberg, F. Biraben, E. Giacobino, and B. Cagnac, J. Phys. **38**, 629 (1977).

[35] J.-Ph. Karr, F. Bielsa, A. Douillet, J. Pedregosa Gutierrez, V.I. Korobov, and L. Hilico, Phys. Rev. A **77**, 063410 (2008).
[36] V.I. Korobov, Mol. Phys. **116**, 93 (2017).
[37] F. von Busch and G.H. Dunn, Phys. Rev. A **5**, 1726 (1972).
[38] P. Perez *et al.*, Hyperfine Interact. **233**, 21 (2015).
[39] See Supplemental Material at ... for the values of the two-photon matrix elements.
[40] L. Hilico, N. Billy, B. Grémaud, and D. Delande, J. Phys. B **34**, 1 (2001).
[41] J.A. Smith, S. Hamzeloui, D.J. Fink, and E.G. Myers, Phys. Rev. Lett. **120**, 143002 (2018).

TABLE I: Averaged decay rates $\bar{A}_{v,L,v',L'}/(B_0^4 r_c^2)$ in $\mathrm{s}^{-1}\mathrm{T}^{-4}\mathrm{mm}^{-2}$ with $v' = v$, $L' = L - 2$.

L/v	0	1	2	3	4	5	6	7	8	9	10	11	12
2	6.693E-14	1.154E-13	1.911E-13	3.085E-13	4.896E-13	7.703E-13	1.209E-12	1.904E-12	3.029E-12	4.900E-12	8.124E-12	1.395E-11	2.517E-11
3	3.996E-13	6.882E-13	1.139E-12	1.838E-12	2.918E-12	4.591E-12	7.207E-12	1.136E-11	1.808E-11	2.928E-11	4.861E-11	8.366E-11	
4	1.224E-12	2.105E-12	3.482E-12	5.615E-12	8.912E-12	1.402E-11	2.203E-11	3.474E-11	5.537E-11	8.981E-11	1.495E-10	2.580E-10	
5	2.774E-12	4.765E-12	7.875E-12	1.269E-11	2.014E-11	3.170E-11	4.983E-11	7.868E-11	1.256E-10	2.042E-10	3.409E-10		
6	5.299E-12	9.084E-12	1.500E-11	2.416E-11	3.833E-11	6.035E-11	9.494E-11	1.501E-10	2.402E-10	3.916E-10	6.564E-10		
7	9.062E-12	1.550E-11	2.556E-11	4.114E-11	6.527E-11	1.028E-10	1.620E-10	2.566E-10	4.116E-10	6.735E-10			
8	1.435E-11	2.448E-11	4.031E-11	6.485E-11	1.029E-10	1.623E-10	2.559E-10	4.064E-10	6.539E-10	1.075E-09			
9	2.146E-11	3.653E-11	6.007E-11	9.660E-11	1.533E-10	2.420E-10	3.824E-10	6.089E-10	9.836E-10				
10	3.075E-11	5.221E-11	8.574E-11	1.378E-10	2.189E-10	3.459E-10	5.479E-10	8.752E-10	1.420E-09				
11	4.259E-11	7.214E-11	1.183E-10	1.902E-10	3.022E-10	4.785E-10	7.599E-10	1.219E-09					
12	5.741E-11	9.703E-11	1.590E-10	2.555E-10	4.066E-10	6.451E-10	1.028E-09	1.656E-09					
13	7.569E-11	1.277E-10	2.090E-10	3.361E-10	5.355E-10	8.519E-10	1.363E-09						
14	9.800E-11	1.650E-10	2.700E-10	4.345E-10	6.936E-10	1.107E-09	1.779E-09						
15	1.250E-10	2.101E-10	3.437E-10	5.538E-10	8.862E-10	1.420E-09							
16	1.573E-10	2.641E-10	4.323E-10	6.977E-10	1.120E-09	1.802E-09							
17	1.959E-10	3.287E-10	5.384E-10	8.708E-10	1.403E-09	2.270E-09							
18	2.417E-10	4.055E-10	6.651E-10	1.079E-09	1.746E-09								
19	2.959E-10	4.965E-10	8.161E-10	1.328E-09	2.161E-09								
20	3.599E-10	6.044E-10	9.959E-10	1.628E-09									
21	4.352E-10	7.320E-10	1.210E-09	1.989E-09									
22	5.238E-10	8.831E-10	1.466E-09										
23	6.279E-10	1.062E-09	1.772E-09										
24	7.503E-10	1.274E-09											
25	8.942E-10	1.526E-09											
26	1.064E-09												
27	1.264E-09												

TABLE II: Same as Table I, with $v' = v - 1$.

L/v	1	2	3	4	5	6	7	8	9	10	11	12
2	2.819E-11	7.437E-11	1.476E-10	2.618E-10	4.384E-10	7.110E-10	1.134E-09	1.798E-09	2.857E-09	4.584E-09	7.489E-09	1.259E-08
3	3.959E-11	1.042E-10	2.066E-10	3.659E-10	6.122E-10	9.926E-10	1.583E-09	2.511E-09	3.990E-09	6.408E-09	1.048E-08	
4	4.789E-11	1.258E-10	2.489E-10	4.404E-10	7.362E-10	1.193E-09	1.903E-09	3.019E-09	4.802E-09	7.721E-09	1.266E-08	
5	5.512E-11	1.445E-10	2.855E-10	5.044E-10	8.426E-10	1.365E-09	2.177E-09	3.455E-09	5.502E-09	8.860E-09		
6	6.198E-11	1.621E-10	3.197E-10	5.643E-10	9.418E-10	1.525E-09	2.434E-09	3.865E-09	6.162E-09	9.943E-09		
7	6.876E-11	1.794E-10	3.533E-10	6.228E-10	1.039E-09	1.682E-09	2.685E-09	4.269E-09	6.817E-09			
8	7.564E-11	1.970E-10	3.871E-10	6.818E-10	1.137E-09	1.841E-09	2.940E-09	4.680E-09	7.488E-09			
9	8.274E-11	2.150E-10	4.219E-10	7.424E-10	1.237E-09	2.004E-09	3.204E-09	5.108E-09				
10	9.016E-11	2.338E-10	4.582E-10	8.056E-10	1.343E-09	2.176E-09	3.482E-09	5.562E-09				
11	9.800E-11	2.537E-10	4.965E-10	8.725E-10	1.454E-09	2.359E-09	3.780E-09					
12	1.063E-10	2.748E-10	5.374E-10	9.440E-10	1.574E-09	2.555E-09	4.103E-09					
13	1.153E-10	2.975E-10	5.814E-10	1.021E-09	1.704E-09	2.770E-09						
14	1.250E-10	3.221E-10	6.291E-10	1.105E-09	1.845E-09	3.005E-09						
15	1.355E-10	3.489E-10	6.812E-10	1.197E-09	2.002E-09							
16	1.470E-10	3.782E-10	7.386E-10	1.299E-09	2.176E-09							
17	1.596E-10	4.105E-10	8.021E-10	1.413E-09	2.370E-09							
18	1.735E-10	4.463E-10	8.727E-10	1.539E-09								
19	1.889E-10	4.862E-10	9.516E-10	1.681E-09								
20	2.060E-10	5.307E-10	1.040E-09									
21	2.252E-10	5.806E-10	1.140E-09									
22	2.466E-10	6.368E-10										
23	2.708E-10	7.003E-10										
24	2.980E-10											
25	3.288E-10											

TABLE III: Same as Table I, with $v' = v - 2$.

L/v	2	3	4	5	6	7	8	9	10	11	12
2	1.874E-12	6.880E-12	1.704E-11	3.562E-11	6.787E-11	1.223E-10	2.129E-10	3.628E-10	6.114E-10	1.028E-09	1.739E-09
3	2.072E-12	7.608E-12	1.886E-11	3.945E-11	7.522E-11	1.356E-10	2.362E-10	4.024E-10	6.777E-10	1.138E-09	
4	1.958E-12	7.197E-12	1.786E-11	3.741E-11	7.143E-11	1.290E-10	2.247E-10	3.829E-10	6.445E-10	1.080E-09	
5	1.745E-12	6.426E-12	1.598E-11	3.355E-11	6.418E-11	1.160E-10	2.024E-10	3.451E-10	5.804E-10		
6	1.503E-12	5.550E-12	1.385E-11	2.915E-11	5.591E-11	1.013E-10	1.770E-10	3.018E-10	5.073E-10		
7	1.260E-12	4.674E-12	1.171E-11	2.475E-11	4.764E-11	8.657E-11	1.515E-10	2.584E-10			
8	1.032E-12	3.849E-12	9.697E-12	2.060E-11	3.983E-11	7.262E-11	1.273E-10	2.172E-10			
9	8.236E-13	3.097E-12	7.863E-12	1.682E-11	3.269E-11	5.984E-11	1.051E-10				
10	6.392E-13	2.430E-12	6.231E-12	1.344E-11	2.630E-11	4.836E-11	8.507E-11				
11	4.797E-13	1.851E-12	4.807E-12	1.048E-11	2.068E-11	3.819E-11					
12	3.447E-13	1.358E-12	3.587E-12	7.929E-12	1.579E-11	2.931E-11					
13	2.337E-13	9.471E-13	2.562E-12	5.763E-12	1.161E-11						
14	1.455E-13	6.154E-13	1.721E-12	3.963E-12	8.096E-12						
15	7.890E-14	3.581E-13	1.053E-12	2.508E-12							
16	3.296E-14	1.715E-13	5.512E-13	1.384E-12							
17	6.870E-15	5.313E-14	2.096E-13	5.839E-13							
18	2.459E-16	2.122E-15	2.878E-14								
19	1.320E-14	1.988E-14	1.580E-14								
20	4.654E-14	1.108E-13									
21	1.019E-13	2.832E-13									
22	1.822E-13										
23	2.917E-13										

TABLE IV: Averaged decay rates $\bar{A}_{v,L,v',L'}/(B_0^4 r_c^2)$ in $\mathrm{s}^{-1}\mathrm{T}^{-4}\mathrm{mm}^{-2}$ with $v' = v - 1$, $L' = L$.

L/v	1	2	3	4	5	6	7	8	9	10	11	12
0	1.298E-10	3.033E-10	5.405E-10	8.716E-10	1.343E-09	2.027E-09	3.040E-09	4.576E-09	6.963E-09	1.079E-08	1.713E-08	2.816E-08
1	1.794E-10	4.344E-10	8.014E-10	1.335E-09	2.120E-09	3.289E-09	5.055E-09	7.771E-09	1.204E-08	1.893E-08	3.044E-08	5.052E-08
2	1.665E-10	4.003E-10	7.335E-10	1.215E-09	1.918E-09	2.962E-09	4.536E-09	6.952E-09	1.075E-08	1.688E-08	2.713E-08	4.505E-08
3	1.659E-10	3.986E-10	7.301E-10	1.209E-09	1.909E-09	2.948E-09	4.516E-09	6.928E-09	1.072E-08	1.687E-08	2.717E-08	
4	1.673E-10	4.024E-10	7.376E-10	1.222E-09	1.932E-09	2.988E-09	4.584E-09	7.045E-09	1.093E-08	1.723E-08	2.785E-08	
5	1.698E-10	4.089E-10	7.506E-10	1.246E-09	1.973E-09	3.056E-09	4.699E-09	7.239E-09	1.126E-08	1.782E-08		
6	1.731E-10	4.175E-10	7.678E-10	1.277E-09	2.026E-09	3.147E-09	4.852E-09	7.497E-09	1.170E-08	1.860E-08		
7	1.771E-10	4.281E-10	7.891E-10	1.315E-09	2.093E-09	3.260E-09	5.041E-09	7.819E-09	1.226E-08			
8	1.819E-10	4.407E-10	8.144E-10	1.361E-09	2.172E-09	3.395E-09	5.270E-09	8.209E-09	1.294E-08			
9	1.874E-10	4.553E-10	8.438E-10	1.415E-09	2.266E-09	3.554E-09	5.541E-09	8.673E-09				
10	1.937E-10	4.721E-10	8.778E-10	1.477E-09	2.375E-09	3.741E-09	5.860E-09	9.223E-09				
11	2.008E-10	4.911E-10	9.165E-10	1.548E-09	2.500E-09	3.957E-09	6.232E-09					
12	2.089E-10	5.127E-10	9.606E-10	1.630E-09	2.644E-09	4.207E-09	6.666E-09					
13	2.179E-10	5.370E-10	1.010E-09	1.722E-09	2.809E-09	4.496E-09						
14	2.280E-10	5.643E-10	1.067E-09	1.828E-09	2.998E-09	4.829E-09						
15	2.392E-10	5.949E-10	1.131E-09	1.948E-09	3.214E-09							
16	2.517E-10	6.292E-10	1.202E-09	2.084E-09	3.462E-09							
17	2.657E-10	6.677E-10	1.283E-09	2.239E-09	3.748E-09							
18	2.812E-10	7.109E-10	1.375E-09	2.416E-09								
19	2.985E-10	7.594E-10	1.479E-09	2.619E-09								
20	3.178E-10	8.139E-10	1.597E-09									
21	3.394E-10	8.754E-10	1.731E-09									
22	3.636E-10	9.449E-10										
23	3.907E-10	1.024E-09										
24	4.211E-10											
25	4.554E-10											

TABLE V: Same as Table IV, with $v' = v - 2$.

L/v	2	3	4	5	6	7	8	9	10	11	12
0	1.717E-12	7.717E-12	2.265E-11	5.468E-11	1.178E-10	2.360E-10	4.500E-10	8.297E-10	1.497E-09	2.669E-09	4.748E-09
1	6.366E-12	2.480E-11	6.501E-11	1.433E-10	2.867E-10	5.404E-10	9.804E-10	1.735E-09	3.026E-09	5.249E-09	9.135E-09
2	5.116E-12	2.024E-11	5.376E-11	1.199E-10	2.424E-10	4.613E-10	8.435E-10	1.503E-09	2.638E-09	4.600E-09	8.045E-09
3	5.001E-12	1.985E-11	5.291E-11	1.183E-10	2.399E-10	4.574E-10	8.381E-10	1.497E-09	2.631E-09	4.597E-09	
4	5.063E-12	2.013E-11	5.374E-11	1.203E-10	2.443E-10	4.664E-10	8.558E-10	1.530E-09	2.694E-09	4.716E-09	
5	5.207E-12	2.073E-11	5.539E-11	1.242E-10	2.523E-10	4.823E-10	8.858E-10	1.586E-09	2.797E-09		
6	5.412E-12	2.157E-11	5.768E-11	1.294E-10	2.632E-10	5.037E-10	9.263E-10	1.661E-09	2.934E-09		
7	5.673E-12	2.263E-11	6.057E-11	1.360E-10	2.770E-10	5.306E-10	9.771E-10	1.755E-09			
8	5.992E-12	2.392E-11	6.410E-11	1.441E-10	2.937E-10	5.633E-10	1.039E-09	1.869E-09			
9	6.373E-12	2.547E-11	6.830E-11	1.537E-10	3.136E-10	6.024E-10	1.113E-09				
10	6.823E-12	2.729E-11	7.327E-11	1.651E-10	3.373E-10	6.488E-10	1.201E-09				
11	7.350E-12	2.943E-11	7.909E-11	1.784E-10	3.650E-10	7.034E-10					
12	7.964E-12	3.192E-11	8.589E-11	1.940E-10	3.976E-10	7.676E-10					
13	8.677E-12	3.482E-11	9.381E-11	2.122E-10	4.356E-10						
14	9.504E-12	3.819E-11	1.030E-10	2.334E-10	4.800E-10						
15	1.046E-11	4.209E-11	1.137E-10	2.581E-10							
16	1.157E-11	4.661E-11	1.261E-10	2.868E-10							
17	1.285E-11	5.186E-11	1.406E-10	3.203E-10							
18	1.434E-11	5.796E-11	1.574E-10								
19	1.606E-11	6.503E-11	1.770E-10								
20	1.806E-11	7.327E-11									
21	2.039E-11	8.286E-11									
22	2.309E-11										
23	2.623E-11										

TABLE VI: Averaged decay rates $\bar{A}_{v,L,v',L'}/(B_0^4 r_c^2)$ in $\mathrm{s}^{-1}\mathrm{T}^{-4}\mathrm{mm}^{-2}$ with $v' = v-1$, $L' = L+2$. Stars indicate cases where the $(v-1, L+2)$ level lies above the (v, L) level. In these cases, the "reversed" decay rate $\bar{A}_{v',L',v,L}/(B_0^4 r_c^2)$ is given instead.

L/v	1	2	3	4	5	6	7	8	9	10	11	12
0	1.056E-10	2.798E-10	5.574E-10	9.913E-10	1.663E-09	2.701E-09	4.312E-09	6.835E-09	1.085E-08	1.739E-08	2.835E-08	4.750E-08
1	5.695E-11	1.511E-10	3.013E-10	5.362E-10	9.001E-10	1.462E-09	2.335E-09	3.701E-09	5.875E-09	9.412E-09	1.534E-08	2.570E-08
2	4.364E-11	1.159E-10	2.312E-10	4.117E-10	6.913E-10	1.123E-09	1.794E-09	2.843E-09	4.513E-09	7.230E-09	1.178E-08	1.974E-08
3	3.590E-11	9.539E-11	1.904E-10	3.391E-10	5.695E-10	9.255E-10	1.478E-09	2.342E-09	3.717E-09	5.953E-09	9.702E-09	
4	3.024E-11	8.036E-11	1.604E-10	2.857E-10	4.798E-10	7.796E-10	1.244E-09	1.972E-09	3.129E-09	5.009E-09	8.162E-09	
5	2.566E-11	6.820E-11	1.361E-10	2.424E-10	4.069E-10	6.609E-10	1.054E-09	1.670E-09	2.648E-09	4.237E-09		
6	2.179E-11	5.788E-11	1.155E-10	2.055E-10	3.448E-10	5.596E-10	8.921E-10	1.412E-09	2.236E-09	3.573E-09		
7	1.843E-11	4.891E-11	9.751E-11	1.734E-10	2.905E-10	4.710E-10	7.499E-10	1.185E-09	1.874E-09			
8	1.548E-11	4.103E-11	8.170E-11	1.450E-10	2.427E-10	3.928E-10	6.240E-10	9.837E-10	1.551E-09			
9	1.288E-11	3.408E-11	6.772E-11	1.200E-10	2.003E-10	3.234E-10	5.123E-10	8.046E-10				
10	1.058E-11	2.794E-11	5.539E-11	9.787E-11	1.629E-10	2.619E-10	4.131E-10	6.454E-10				
11	8.568E-12	2.255E-11	4.455E-11	7.840E-11	1.299E-10	2.078E-10	3.256E-10					
12	6.809E-12	1.785E-11	3.509E-11	6.142E-11	1.011E-10	1.605E-10	2.491E-10					
13	5.288E-12	1.378E-11	2.692E-11	4.676E-11	7.627E-11	1.197E-10						
14	3.990E-12	1.032E-11	1.997E-11	3.432E-11	5.523E-11	8.525E-11						
15	2.901E-12	7.421E-12	1.418E-11	2.398E-11	3.784E-11							
16	2.010E-12	5.061E-12	9.489E-12	1.567E-11	2.399E-11							
17	1.303E-12	3.207E-12	5.841E-12	9.294E-12	1.353E-11							
18	7.696E-13	1.826E-12	3.172E-12	4.739E-12								
19	3.939E-13	8.781E-13	1.402E-12	1.858E-12								
20	1.583E-13	3.124E-13	4.173E-13									
21	3.880E-14	5.593E-14	4.244E-14									
22	1.911E-15	2.881E-16										
23	9.695E-16*	1.756E-14*										
24	3.659E-14*											
25	1.999E-13*											

TABLE VII: Same as Table VI, with $v' = v - 2$.

L/v	2	3	4	5	6	7	8	9	10	11	12
0	1.392E-11	5.119E-11	1.269E-10	2.654E-10	5.057E-10	9.117E-10	1.588E-09	2.712E-09	4.587E-09	7.753E-09	1.322E-08
1	9.373E-12	3.450E-11	8.562E-11	1.792E-10	3.417E-10	6.165E-10	1.075E-09	1.838E-09	3.114E-09	5.275E-09	9.023E-09
2	8.947E-12	3.298E-11	8.194E-11	1.717E-10	3.277E-10	5.918E-10	1.033E-09	1.769E-09	3.003E-09	5.102E-09	8.759E-09
3	9.163E-12	3.383E-11	8.416E-11	1.765E-10	3.374E-10	6.102E-10	1.067E-09	1.830E-09	3.115E-09	5.307E-09	
4	9.614E-12	3.555E-11	8.858E-11	1.861E-10	3.561E-10	6.451E-10	1.130E-09	1.943E-09	3.315E-09	5.668E-09	
5	1.018E-11	3.772E-11	9.415E-11	1.981E-10	3.798E-10	6.891E-10	1.210E-09	2.085E-09	3.568E-09		
6	1.083E-11	4.018E-11	1.004E-10	2.117E-10	4.066E-10	7.393E-10	1.301E-09	2.249E-09	3.862E-09		
7	1.152E-11	4.283E-11	1.073E-10	2.265E-10	4.360E-10	7.945E-10	1.402E-09	2.430E-09			
8	1.225E-11	4.565E-11	1.145E-10	2.424E-10	4.675E-10	8.541E-10	1.511E-09	2.630E-09			
9	1.302E-11	4.860E-11	1.222E-10	2.591E-10	5.011E-10	9.179E-10	1.629E-09				
10	1.382E-11	5.168E-11	1.302E-10	2.768E-10	5.366E-10	9.860E-10	1.756E-09				
11	1.464E-11	5.489E-11	1.386E-10	2.954E-10	5.743E-10	1.059E-09					
12	1.550E-11	5.823E-11	1.474E-10	3.150E-10	6.141E-10	1.136E-09					
13	1.639E-11	6.171E-11	1.566E-10	3.356E-10	6.564E-10						
14	1.732E-11	6.535E-11	1.663E-10	3.573E-10	7.013E-10						
15	1.828E-11	6.915E-11	1.764E-10	3.803E-10							
16	1.928E-11	7.312E-11	1.871E-10	4.046E-10							
17	2.032E-11	7.728E-11	1.983E-10	4.303E-10							
18	2.141E-11	8.165E-11	2.102E-10								
19	2.255E-11	8.622E-11	2.226E-10								
20	2.374E-11	9.101E-11									
21	2.498E-11	9.601E-11									
22	2.626E-11										
23	2.758E-11										

TABLE VIII: Total decay rates $\bar{A}_{v,L}/(B_0^4 r_c^2)$ in $\mathrm{s}^{-1}\mathrm{T}^{-4}\mathrm{mm}^{-2}$.

L/v	0	1	2	3	4	5	6	7	8	9	10	11	12
0	0	2.353E-10	5.987E-10	1.157E-09	2.013E-09	3.327E-09	5.354E-09	8.503E-09	1.346E-08	2.136E-08	3.427E-08	5.592E-08	9.367E-08
1	0	2.363E-10	6.013E-10	1.162E-09	2.022E-09	3.343E-09	5.381E-09	8.549E-09	1.353E-08	2.150E-08	3.450E-08	5.633E-08	9.442E-08
2	6.693E-14	2.384E-10	6.067E-10	1.173E-09	2.042E-09	3.377E-09	5.438E-09	8.644E-09	1.369E-08	2.177E-08	3.497E-08	5.717E-08	9.599E-08
3	3.996E-13	2.420E-10	6.156E-10	1.190E-09	2.073E-09	3.430E-09	5.528E-09	8.795E-09	1.395E-08	2.220E-08	3.571E-08	5.850E-08	
4	1.224E-12	2.475E-10	6.286E-10	1.216E-09	2.118E-09	3.507E-09	5.656E-09	9.010E-09	1.431E-08	2.281E-08	3.678E-08	6.041E-08	
5	2.774E-12	2.553E-10	6.466E-10	1.250E-09	2.178E-09	3.610E-09	5.830E-09	9.299E-09	1.479E-08	2.364E-08	3.822E-08		
6	5.299E-12	2.659E-10	6.702E-10	1.295E-09	2.257E-09	3.744E-09	6.054E-09	9.674E-09	1.542E-08	2.471E-08	4.010E-08		
7	9.062E-12	2.798E-10	7.005E-10	1.351E-09	2.357E-09	3.913E-09	6.337E-09	1.015E-08	1.622E-08	2.608E-08			
8	1.435E-11	2.975E-10	7.383E-10	1.422E-09	2.479E-09	4.122E-09	6.687E-09	1.073E-08	1.721E-08	2.778E-08			
9	2.146E-11	3.195E-10	7.847E-10	1.507E-09	2.629E-09	4.376E-09	7.114E-09	1.145E-08	1.843E-08				
10	3.075E-11	3.466E-10	8.408E-10	1.611E-09	2.809E-09	4.682E-09	7.629E-09	1.232E-08	1.991E-08				
11	4.259E-11	3.795E-10	9.081E-10	1.734E-09	3.024E-09	5.048E-09	8.246E-09	1.336E-08					
12	5.741E-11	4.190E-10	9.881E-10	1.880E-09	3.279E-09	5.482E-09	8.982E-09	1.462E-08					
13	7.569E-11	4.661E-10	1.083E-09	2.053E-09	3.580E-09	5.996E-09	9.857E-09						
14	9.800E-11	5.219E-10	1.194E-09	2.255E-09	3.933E-09	6.603E-09	1.090E-08						
15	1.250E-10	5.876E-10	1.324E-09	2.492E-09	4.348E-09	7.318E-09							
16	1.573E-10	6.648E-10	1.476E-09	2.768E-09	4.834E-09	8.162E-09							
17	1.959E-10	7.552E-10	1.653E-09	3.092E-09	5.405E-09	9.159E-09							
18	2.417E-10	8.609E-10	1.860E-09	3.470E-09	6.076E-09								
19	2.959E-10	9.843E-10	2.101E-09	3.912E-09	6.866E-09								
20	3.599E-10	1.128E-09	2.383E-09	4.431E-09									
21	4.352E-10	1.297E-09	2.712E-09	5.040E-09									
22	5.238E-10	1.493E-09	3.097E-09										
23	6.279E-10	1.723E-09	3.550E-09										
24	7.503E-10	1.993E-09											
25	8.942E-10	2.311E-09											
26	1.064E-09												
27	1.264E-09												